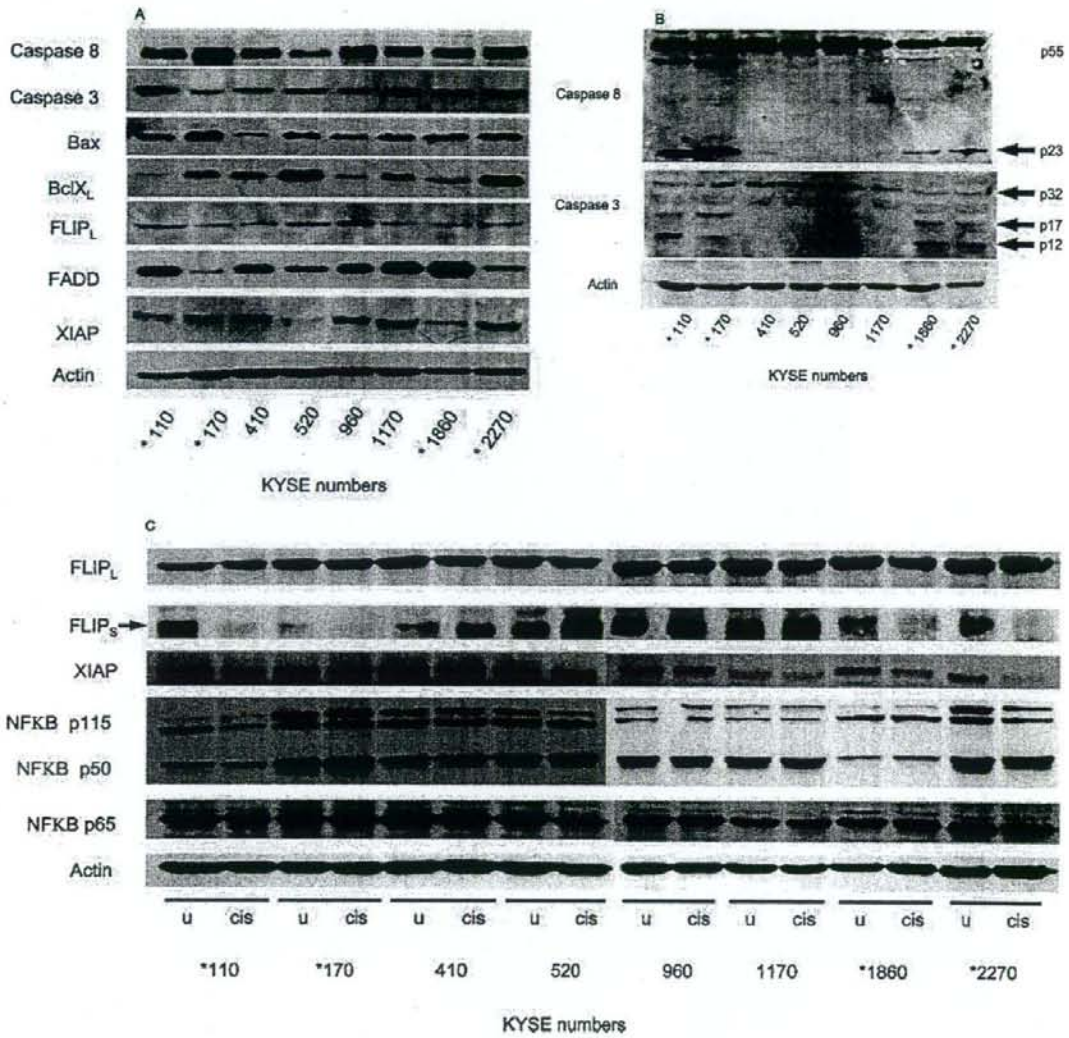

FIGURE 7 – Detection of key apoptotic proteins by immunoblotting analyses: (*a*) in untreated cells, procaspase-8, procaspase-3, Bax, Bcl-XL, cFLIP, FADD and XIAP were expressed in all 8 cell lines. The numbers below the figure represent the cell line numbers. (*b*) Eight hours after the combination treatment with TRAIL and cisplatin, proteolytic activation of procaspase-8 and procaspase-3 were observed in sensitive cell lines KYSE 110, 170, 1860 and 2270 but not in resistant cell lines KYSE 410, 520, 960 and 1170. (*c*) Eight hours after the treatment with 5 μg/ml cisplatin, slight decreases in expression level of anti-apoptotic proteins XIAP and FLIPS were observed in sensitive cell lines. Expression levels of NFκB (p115, p65 and ad p50) remained unchanged. u: untreated samples, cis: samples treated with 5 μg/ml cisplatin, p55: Procaspase-8, p23: cleaved caspase-8, p32: Procaspase-3, p17/p12: cleaved caspase-3. Beta-actin expression is shown as a loading control. Experiments were repeated at least 3 times, and the most representative results are shown. Asterisk denotes cell lines sensitive to the combination treatment.

cant cytotoxicity was observed regardless of the treatment sequence, but in other 3 cell lines, pretreatment with cisplatin followed by treatment with TRAIL resulted in significantly more cytotoxic effects than when the sequence was reversed (Fig. 9).

In vivo *suppression of tumor growth by the treatment of nude mice with TRAIL and cisplatin*

Because cisplatin enhanced the apoptosis-inducing potential of TRAIL by upregulating DR4/5 *in vitro*, we sought to examine whether this combination is effective in an established ESCC tumor model *in vivo*. KYSE 170 was implanted into the right thigh of the nude mice. Similar to *in vitro* experiments, TRAIL and cisplatin were simultaneously injected i.p. to observe their effects. KYSE 170 tumors carried by mice treated with the combination of TRAIL and cisplatin grew slower after the first course of treatment and remained smaller than any other tumors except those treated with 3 mg/kg cisplatin (Fig. 10*a*). In contrast, tumors in mice treated with normal saline or with TRAIL singly grew significantly faster. The suppression of tumor growth by the combination

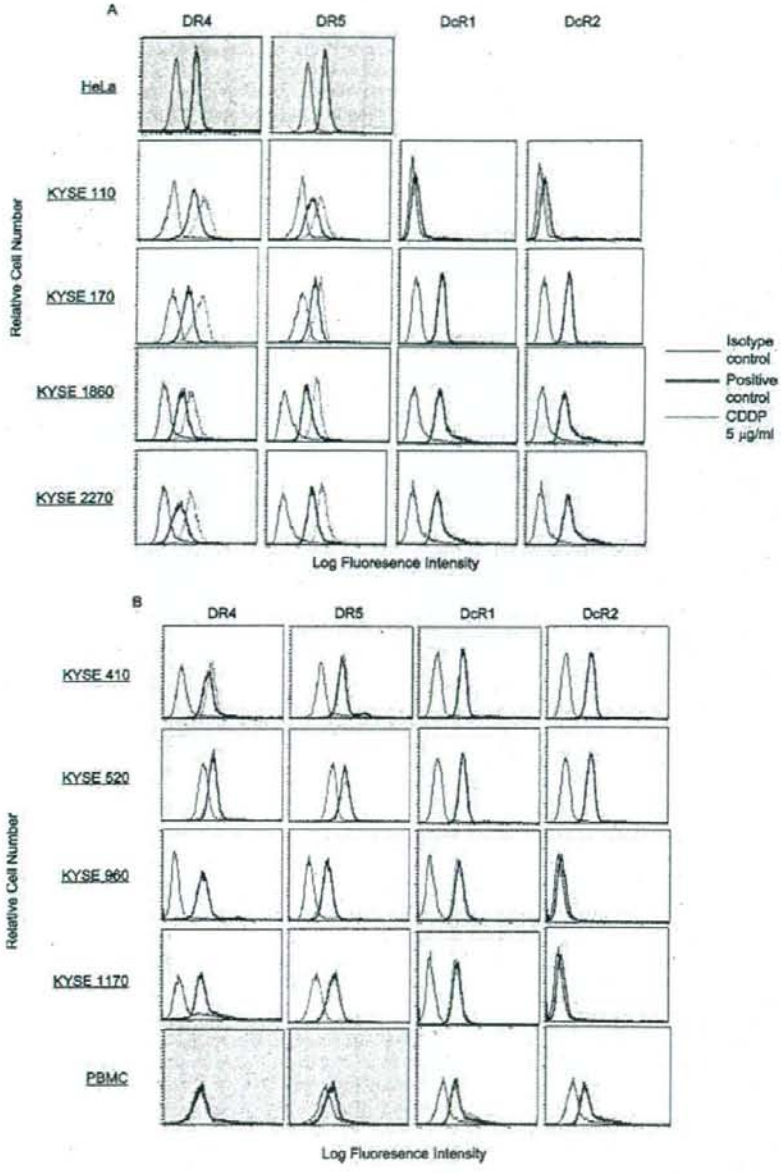

FIGURE 8 – Flow cytometric analysis of surface DR4 and DR5 expression. (*a*) Cell lines sensitive to the combination treatment. (*b*) Cell lines resistant to the combination treatment. HeLa cells served as the positive control for the surface expression of DR4 and DR5. PBMCs served as the positive control for DcR1 and DcR2. The baseline expression patterns of TRAIL receptors in KYSE cell lines paralleled those of the mRNA transcripts. In PBMCs, however, the surface expression of DR4 could not be detected. The cell lines sensitive to the combination treatment revealed cisplatin-induced upregulation of both DR4 and DR5 but in the resistant cell lines including PBMCs, expression levels of DRs was unaffected. Expression of decoy receptors was not influenced by the addition of cisplatin in any of the cell lines. Experiments were repeated at least 3 times for each cell line, and the most representative results are shown.

treatment was statistically significant compared to TRAIL alone ($p = 0.0006$) or normal saline ($p < 0.0005$), but the statistical significance was not reached when compared to the effect of 2 mg/kg cisplatin ($p = 0.253$). On the contrary, weight loss of the mice treated with 3 mg/kg cisplatin was much more than mice in any other groups, though statistical significance was not reached (Fig. 10*b*). Both the suppression of tumor growth and weight loss of mice were dose dependent for cisplatin, but the addition of TRAIL did not appear to influence the weight of mice, consistent with other reports that TRAIL causes minimal or no side effects in mice.[19,32]

Discussion

The present results indicate that ESCC cell lines are generally resistant to TRAIL, but in some cell lines that resistance can be overcome by adding cisplatin. Death signals originate from the

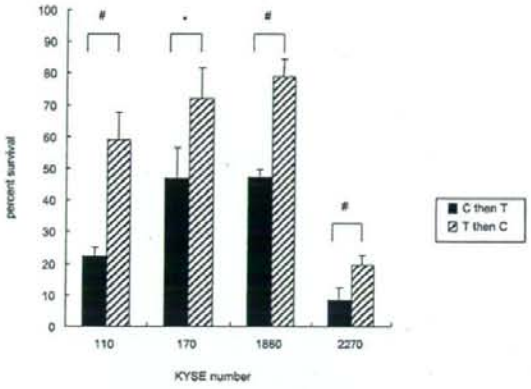

FIGURE 9 – KYSE 110, 170, 1860 and 2270 were subjected to the sequential administration of cisplatin and TRAIL. They were either pretreated with 5 μg/ml cisplatin for 12 hr, followed by treatment with 50 ng/ml TRAIL for 12 hr (C then T), or *vice versa* (T then C), stained with the crystal violet solution and OD absorbance was measured. OD absorbance of untreated cells was set for 100%. For all 4 cell lines, pretreatment with cisplatin followed by TRAIL resulted in statistically significant cytotoxic effects compared to the reverse sequence. KYSE 2270, which is sensitive to TRAIL, revealed significant cytotoxicity regardless of the treatment sequence. Graphs represent the mean of 8 independent experiments for each cell line; bars, SE. #$p < 0.001$. *$p < 0.005$.

TRAIL receptors and we have demonstrated that cisplatin can upregulate DR4/5 to enhance ligand-induced cytotoxicity. All KYSE cell lines expressed both DR4 and DR5, showing a quintessential pattern of death receptor expression in malignant cell lines. The decoy receptors had been thought to play a cytoprotective role against TRAIL in normal cells[3–6,9,10] until TRAIL-sensitive tumors expressing decoy receptors were reported[13,14,20,29,33] to keep their roles remain ambiguous. When compared to other tumor cell lines, incidences of DcR1/2 expression in KYSE cell lines are higher than expected, with only 1 decoy-receptor negative cell line. High incidences of decoy receptor expression may be one of the unique molecular characteristics reflecting TRAIL-resistant nature of ESCC.

Statistical analysis of clinicopathological data of the original cancers revealed that sensitivity to the combination treatment was unrelated to age, gender, location of the tumor, lymph node metastasis, distant lymph node metastasis or TNM staging of the tumor. However, although statistical significant was not reached, well-differentiated ESCC tended to be more resistant to the combination treatment compared to moderately and poorly differentiated ESCC. One of the possible explanations for this is that well differentiated ESCC retains more characteristics of normal esophageal epithelial cells. Since normal cells are generally resistant to TRAIL, well-differentiated ESCC might remain more resistant to the treatment with TRAIL. Furthermore, although statistical significance was not reached, 100 % of the well-differentiated tumors expressed both DcR1 and DcR2 whereas some of the moderately and poorly differentiated tumors lacked decoy receptor expression. By increasing the number of samples, resistant characteristics and differences in expression levels of decoy receptors may become more evident.

Several chemotherapeutic agents including cisplatin, one of the most common anticancer drugs against ESCC, have been reported to upregulate DR4/5 to augment TRAIL-mediated apoptosis in cancer cells.[19,21,22,32] Consequently, we selected cisplatin to evaluate whether or not it can break TRAIL resistance in ESCC. Although cisplatin alone was largely ineffective at the given dose, when combined with TRAIL, synergistic cytotoxicity was exerted in 7 out of 19 (37%) cell lines. Further examination revealed that the addition of cisplatin did not influence decoy receptor expression, but it was rather capable of upregulating DR4/5 to augment TRAIL-mediated apoptosis. Following the time course of death receptor upregulation in these cell lines with flow cytometry, they became clearly bright after 6 hr, but even after the 4 hr contact, the upregulation seemed to have begun (data not shown). These results demonstrated that upregulation of DR4/5 by cisplatin begins relatively early in the sensitive cell lines. However, DR expression of the resistant cell lines was not affected. Several different mechanisms have been suggested for upregulation of DRs. Sheikh *et al.*[34] has shown the involvement of p53 at the transcriptional level in upregulation of DR5, and Gibson *et al.*[22] has suggested differential activation of NFκB could upregulate both DR4 and DR5. Still others suggested the involvement of post-translational mechanisms such as stabilization of cellular microtubules,[35] differential translocation of intracellularly stored DRs upon stimulation by the chemotherapeutic agents[33,36] and chemotherapeutic agent-mediated changes in the rate of receptor turnover at the cell surface.[37] Since none of the mechanisms could sufficiently explain DR upregulation in all of the cancers, this mechanism might differ in different types of cancer. In our study, semiquantitative RT-PCR performed on KYSE 110 and 170 also revealed upregulation of DR4/5 transcripts after the treatment with 5 μg/ml cisplatin (data not shown); therefore, an increase in mRNA transcription may be responsible for DR upregulation in ESCC. Interestingly, in PBMCs, DR4 was not expressed on the surface even though DR4 mRNA was detected in RT-PCR, while surface DR5, DcR1 and DcR2 were expressed, as were their respective mRNA transcripts. The expression of these receptors was not influenced by cisplatin. These results indicate that deficient DR4 expression and lack of DR upregulation in addition to the decoy receptors might contribute to PBMCs' resistance to the combination treatment. It appears that the control of DR4 expression is at the post-transcriptional level in PBMCs, and differs from ESCC. Overall, it may be deduced that the induction of death receptor upregulation by cisplatin in esophageal SCC is indicative of their sensitivity to the combination treatment with TRAIL.

In ESCC, DcR1 and DcR2 do not seem to be essential with regard to their sensitivity against TRAIL for following 2 reasons. First, KYSE 110, the decoy receptor negative cell line, is resistant to TRAIL itself. Second, some of the decoy receptor positive cell lines became susceptible to TRAIL in the presence of cisplatin even though their expression of DcR1 and DcR2 are not influenced by cisplatin. It appears that physiological expression levels of DcR1 and DcR2 are not sufficient to interfere with TRAIL-induced apoptosis as was demonstrated in overexpression experiments of the initial reports investigating TRAIL receptors.[3,6,9,13,14,20,29,33] Furthermore, although a possible role of DcR2 as a NFκB activator has been disclosed,[11] functional roles of DcR1 is yet to be elucidated. Taken together, it seems unlikely that signals originating from DcR1/2 upon binding of TRAIL overcome those from DR4/5 in ESCC to inhibit TRAIL-mediated apoptosis, and the mechanisms of TRAIL resistance seemingly resides on the intracellular factors rather than DcR1 and DcR2.

Apoptosis-inducing mechanisms by TRAIL is thought to be similar to its kin, FasL and TRAIL-mediated apoptosis *via* the extrinsic pathway has been delineated by Griffith *et al.* and others.[15,20,23,29] While TRAIL receptor-specific cytoplasmic adapter protein is yet to be discovered, some studies have reported that FADD may act as the adapter protein for TRAIL receptors.[38] Our study clearly indicated the involvement of caspases in TRAIL-mediated apoptosis of ESCC. However, expression of FADD had been variable among ESCC cell lines and its role as an adapter protein for TRAIL receptors remained unclear. Recently, activation of the intrinsic pathway in TRAIL-mediated apoptosis has been described; Bax seems to take a critical pro-apoptotic role while Bcl-XL is an important inhibitory factor in this pathway of

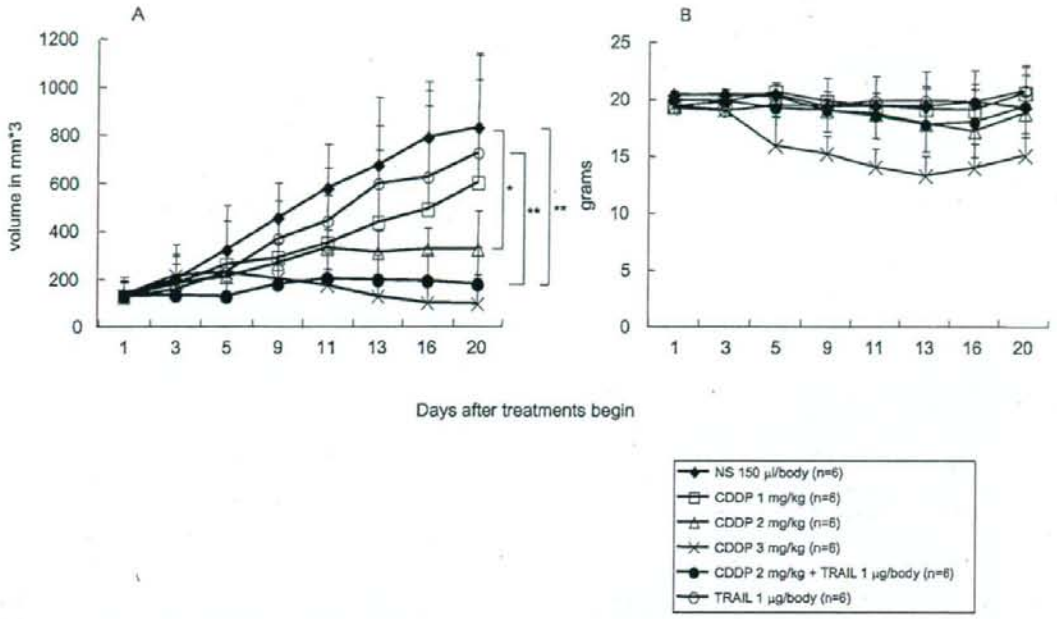

FIGURE 10 – Synergistic antitumor effect of the combination treatment with TRAIL and cisplatin *in vivo*. (*a*) KYSE 170 cells (5×10^6) were inoculated into the right thigh of Balb/c nude mice. After tumor formation, mice received i.p. injection of either TRAIL, cisplatin, normal saline or the combination of TRAIL (1 µg/body) and cisplatin (2 mg/kg). Cisplatin alone induced dose-dependent suppression of xenografted tumor growth, although low-dose cisplatin (1 mg/kg) was largely ineffective. The combination treatment resulted in statistically significant tumor growth suppression compared to both the control and TRAIL-alone groups. (*b*) injection of TRAIL alone resulted in no weight loss of nude mice, while cisplatin caused weight loss of nude mice in a dose-dependent manner. Weight loss was particularly prominent when 3 mg/kg cisplatin was administered. Closed circle, Control group with normal saline; open circle, TRAIL (1 µg/body); open square, cisplatin (1 mg/kg); open triangle, cisplatin (2 mg/kg); ×, cisplatin (3 mg/kg); closed circle, TRAIL (1 µg/kg) + cisplatin (2 mg/kg). Data are shown as the means; bars, SE. $*p < 0.05$. $**p < 0.001$.

apoptosis.[38–42] We detected varying levels of Bax and Bcl-XL in 8 KYSE cell lines but the evidence for the intrinsic pathway activation in the sensitive cell lines could not be obtained. Meanwhile, detection of anti-apoptotic proteins by Western blotting disclosed slight decreases in FLIPS and XIAP expression in the combination-treatment sensitive cell lines after the treatment with 5 µg/ml cisplatin. Such changes were not observed in the resistant KYSE cell lines. FLIP blocks the binding of caspase-8 to the death domains of DR to inhibit apoptosis induction and has been shown to be critical in TRAIL resistance of other cancers,[13,34,43,44] while XIAP inhibits the intrinsic pathway of apoptosis.[45] Cisplatin-mediated decreases of these 2 proteins might partially explain the cell lines' sensitivity to the combination treatment. However, more definitive intracellular mechanisms that determine ESCC's sensitivity to TRAIL and cisplatin are likely to exist, and this shall be the topic of further study. On the contrary, Western blotting did not prove any significant changes in the NFκB expression levels after the cisplatin treatment in any of the cell lines. While NFκB is generally considered anti-apoptotic,[11,46] a moderate amount of activated NFκB has been suggested to upregulate DRs.[22] Subsequently, it will be necessary to detect the active form of NFκB to evaluate its roles in DR upregulation of ESCC.

Importantly, pretreatment of KYSE cell lines with cisplatin followed by TRAIL resulted in significant cytotoxic effects compared to the reverse sequence in the treatment-sensitive KYSE cell lines, thus supporting the significance of cisplatin-induced upregulation of DRs. Furthermore, *in vivo* experiments with nude mice revealed synergistic effects of the combination treatment similar to *in vitro* results when compared to the TRAIL-alone (1 µg/body) group. Although statistical significance was not reached when compared to cisplatin-alone group (2 mg/kg), tendency toward synergy was observed; an encouraging outcome that may lead to further investigation. Notably, we were able to obtain these results with much lower dose of TRAIL than previously reported.[19,32] Growth of the xenografted KYSE 170 was suppressed by administration of cisplatin alone even though this cell line was resistant to cisplatin *in vitro*. We believe this seemingly discrepant result was obtained probably because with the administration of the given concentration of cisplatin, the serum concentration became sufficiently high to cause some apoptosis. TRAIL was shown to have negligible influences on weight loss at 1 µg/body, implying minimal side effects.

These results support the cisplatin-dependent DR upregulation as a critical factor in augmenting TRAIL-mediated apoptosis in ESCC and in addition may provide the following clinical implication: first, there is a possibility that the combination therapy can overcome not only TRAIL resistant but also cisplatin resistant ESCC. Second, synergistic effects of the combination treatment against ESCC obtained *in vitro* can be translated into *in vivo* experiments. Third, in the clinical settings, sequential administration of cisplatin and TRAIL, which may be safer, might be the better way of treating the patients. Since the critical issue regarding toxicity of recombinant human TRAIL to normal human cells appeared to be resolved by alternating its

formulation,[17,18] TRAIL shall remain as a feasible candidate for anticancer therapies. While testing for clinical application of the recombinant human TRAIL against many different cancers is presently under intense investigation, research on TRAIL against ESCC has been limited. We attempted to show such a possibility, and it is our hope that continuing researches may eventually lead to the introduction of TRAIL as the standard agent for anti-esophageal cancer therapy.

References

1. Wiley RS, Schooley K, Smolak PJ, Din WS, Huang C-P, Nicholl JK, Sutherland GR, Smith TD, Rauch C, Smith CA, Goodwin RG. Identification and characterization of a new member of the TNF family that induces apoptosis. Immunity 1995;3:673–82.
2. Pitti RM, Marsters SA, Ruppert S, Donahue CJ, Moore A, Ashkenazi A. Induction of apoptosis by Apo-2 ligand, a new member of the tumor necrosis factor cytokine family. J Biol Chem 1996;271:12687–90.
3. Pan G, O'Rourke K, Chinnaiyan AM, Gentz R, Ebner R, Ni J, Dixit VM. The receptor for the cytotoxic ligand TRAIL. Science 1997; 276:111–3.
4. Schneider P, Bodmer J-L, Thome M, Hofmann K, Holler N, Tschopp J. Characterization of two receptors for TRAIL. FEBS Lett 1997; 416:329–34.
5. Sheridan JP, Marsters SA, Pitti RM, Gurney A, Skubatch M, Baldwin D, Ramakrishnan L, Gray CL, Baker K, Wood WI, Goddard AD, Godowski P, et al. Control of TRAIL-induced apoptosis by a family of signaling and decoy receptors. Science 1997;277:818–21.
6. Pan G, Ni J, Wei Y-F, Yu G-L, Gentz R, Dixit VM. An antagonist decoy receptor and a death domain-containing receptor for TRAIL. Science 1997;277:815–8.
7. Walczak H, Degli-Esposti MA, Johnson RS, Smolak PJ, Waugh JY, Boiani N, Timour MS, Gerhart MJ, Schooley KA, Smith CA, Goodwin RG, Rauch CT. TRAIL-R2: a novel apoptosis-mediating receptor for TRAIL. EMBO J 1997;16:5386–97.
8. Chaundhary PM, Eby M, Jasmin A, Bookwalter A, Murray J, Hood L. Death receptor 5, a new member of the TNFR family, and DR4 induce FADD-dependent apoptosis and activate the NF-κB pathway. Immunity 1997;7:821–30.
9. Marsters SA, Sheridan JP, Pitti RM, Huang A, Skubatch M, Baldwin D, Yuan J, Gurney A, Goddard AD, Godowski P, Ashkenazi A. A novel receptor for Apo2L/TRAIL contains a truncated death domain. Curr Biol 1997;7:1003–6.
10. Pan G, Ni J, Yu G-L, Wei Y-F, Dixit VM. TRUNDD, a new member of the TRAIL receptor family that antagonizes TRAIL signaling. FEBS Lett 1998;424:41–5.
11. Degli-Esposti MA, Dougall WC, Smolak PJ, Waugh JY, Smith CA, Goodwin RG. The novel receptor TRAIL-R4 induces NF-κB and protects against TRAIL-mediated apoptosis, yet retains an incomplete death domain. Immunity 1997;7:813–20.
12. Jo M, Kim T-H, Seol D-W, Esplen JE, Dorko K, Billiar TR, Strom SC. Apoptosis induced in normal human hepatocytes by tumor necrosis factor-related apoptosis-inducing ligand. Nat Med 2000;6: 564–7.
13. Kim K, Fisher MJ, Xu S-Q, El-Deiry WS. Molecular determinants of response to TRAIL in killing of normal and cancer cells. Clin Cancer Res 2000;6:335–46.
14. Keane MM, Ettenberg SA, Nau MM, Russell EK, Lipkowitz S. Chemotherapy augments TRAIL-induced apoptosis in breast cancer cell lines. Cancer Res 1999;59:734–41.
15. Griffith TS, Rauch CT, Smolak PJ, Waugh JY, Boiani N, Lynch DH, Smith CA, Goodwin RG, Kubin MZ. Functional analysis of TRAIL receptors using monoclonal antibodies. J Immunol 1999;162:2597–605.
16. Leverkus M, Neumann M, Mengling T, Rauch CT, Brocker E-B, Krammer PH, Walczak H. Regulation of Tumor necrosis factor-related apoptosis-inducing ligand sensitivity in primary and transformed human keratinocytes. Cancer Res 2000;60:553–9.
17. Qin J-Z, Chaturvedi V, Bonish B, Nickoloff BJ. Avoiding premature apoptosis of normal epidermal cells. Nat Med 2001;7:385–6.
18. Lawrence D, Shahrokh Z, Marsters S, Achilles K, Shih D, Mounho B, Hillan K, Totpal K, DeForge L, Schow P, Hooley J, Sherwood S et al. Differential hepatocyte toxicity of recombinant Apo2L/TRAIL versions. Nat Med 2001;7:383–85.
19. Nagane M, Pan G, Weddle JJ, Dixit VM, Cavenee WK, Su Huang H-J. Increased death receptor 5 expression by chemotherapeutic agents in human gliomas causes synergistic cytotoxicity with tumor necrosis factor-related apoptosis-inducing ligand in vitro and in vivo. Cancer Res 2000;60:847–53.
20. Eggert A, Grotzer MA, Zuzak TJ, Wiewrodt BR, Ho R, Ikegaki N, Brodeur GM. Resistance to Tumor necrosis factor-related apoptosis-inducing ligand-induced apoptosis in neuroblastoma cells correlates with a loss of caspase-8 expression. Cancer Res 2001;61:1314–9.
21. Naka T, Sugamura K, Hylander BL, Widmer MB, Rustum YM, Repasky EA. Effects of tumor necrosis factor-related apoptosis-inducing ligand alone and in combination with chemotherapeutic agents on patients' colon tumors grown in SCID mice. Cancer Res 2002;62: 5800–6.
22. Gibson SB, Oyer R, Spalding AC, Anderson SM, Johnson GL. Increased expression of death receptors 4 and 5 synergizes the apoptosis response to combined treatment with etoposide and TRAIL. Mol Cell Biol 2000;20:205–12.
23. Hopkins-Donaldson S, Bodmer J-L, Bourloud KB, Brognara CB, Tschopp J, Gross N. Loss of caspase-8 expression in highly malignant human neuroblastoma cells correlates with resistance to tumor necrosis factor-related apoptosis-inducing ligand-induced apoptosis. Cancer Res 2000;60:4315–9.
24. Shimada Y, Imamura M, Wagata T, Yamaguchi N, Tobe T. Characterization of 21 newly established esophageal cancer cell lines. Cancer 1992;69:277–84.
25. Kanda Y, Nishiyama Y, Shimada Y, Imamura M, Nomura H, Hiai H, Fukumoto M. Analysis of gene amplification and overexpression in human esophageal-carcinoma cell lines. Int J Cancer 1994;58:291–7.
26. Yu R, Mandlekar S, Ruben S, Ni J, Kong A-NT. Tumor necrosis factor-related apoptosis-inducing ligand-mediated apoptosis in androgen-independent prostate cancer cells. Cancer Res 2000;60:2384–9.
27. Grusch M, Fritzer-Szkeres M, Fuhrmann G, Rosenberger G, Luxbacher C, Elford HL, Smid K, Peters GJ, Szekeres T, Krupitza G. Activation of caspases and induction of apoptosis by novel ribonucleotide reductase inhibitors amidox and didox. Exp Hematol 2001; 29:623–32.
28. Miyahara T, Ueda K, Akaboshi M, Shimada Y, Imamura M, Utsumi H. Hyperthermic enhancement of cytotoxicity and increased uptake of cis-diamminedichloroplatinum(II) in cultured human esophageal cancer cells. Jpn J Cancer Res 1993;84:336–40.
29. Griffith TS, Chin WA, Jackson GC, Lynch DH, Kubin MZ. Intracellular regulation of TRAIL-induced apoptosis in human melanoma cells. J Immunol 1998;161:2833–40.
30. Korsmeyer SJ, Wei MC, Saito M, Weiler S, Oh KJ, Schlesinger PH. Pro-apoptotic cascade activates BID, which oligomerizes BAK or BAX into pores that result in the release of cytochrome c. Cell Death Diff 2000;7:1166–73.
31. Li H, Zhu H, Xu CJ, Yuan J. Cleavage of BID by caspases 8 mediates the mitochondrial damage in the Fas pathway of apoptosis. Cell 1998;94:491–501.
32. Singh TR, Shankar S, Chen X, Asim M, Strivastava RK. Synergistic interactions of chemotherapeutic drugs and Tumor Necrosis Factor-related apoptosis-inducing ligand/Apo-2L ligand on apoptosis and on regression of breast carcinoma in vivo. Cancer Res 2003;63:5390–400.
33. Yamanaka T, Shiraki K, Sugimoto K, Ito T, Fujikawa K, Ito M, Takase K, Moriyama M, Nakano T, Suzuki A. Chemotherapeutic agents augment TRAIL-induced apoptosis in human hepatocellular carcinoma cell lines. Hepatology 2000;32:482–90.
34. Sheikh MS, Burns TF, Huang Y, Wu GS, Amundson S, Brooks KS, Fornace AJ Jr., El-Deiry WS. p53-dependent and -independent regulation of the death receptor KILLER/DR5 gene expression in response to genotoxic stress and tumor necrosis alpha. Cancer Res 1998;58: 1593–8.
35. Nimmanapalli R, Perkins CL, Orlando M, O'Bryan E, Nguyen D, Bhalla KN. Pretreatment with paclitaxel enhances apo-2 ligand/tumor necrosis factor-related apoptosis-inducing ligand-induced apoptosis of prostate cancer cells by inducing death receptors 4 and 5 protein levels. Cancer Res 2001;61:759–63.
36. Zhang XD, Franco AV, Nguyen T, Gray CP, Hersey P. Differential localization of death and decoy receptors for TNF-related apoptosis-inducing ligand (TRAIL) in human melanoma cells. J Immunol 2000;164:3961–70.
37. Griffith TS, Fialkov JM, Scott DL, Azuhata T, Williams RD, Wall NR, Altieri DC, Sandler AD. Induction and regulation of tumor necrosis factor-related apoptosis-inducing ligand/Apo-2 ligand-mediated apoptosis in renal cell carcinoma. Cancer Res 2002;62:3093–9.
38. Suliman A, Lam A, Datta R, Strivastava RK. Intracellular mechanism of TRAIL: apoptosis through mitochondrial-dependent and -independent pathways. Oncogene 2001;20:2221–33.
39. Ravi R, Bedi A. Requirement of BAX for TRAIL/Apo2L-induced apoptosis of colorectal cancers: synergism with Sulindac-mediated inhibition of Bcl-XL. Cancer Res 2002;62:1583–7.
40. Kim J-Y, Kim Y-H, Chang I, Kim S, Pak YK, Oh B-H, Yagita H, Jung YK, Oh YJ, Lee M-S. Resistance of mitochondrial DNA-defi-

cient cells to TRAIL: role of Bax in TRAIL-induces apoptosis. Oncogene 2001;21:3139–48.
41. Sarker M, Ruiz-Ruiz C, Robledo G, López-Rivas A. Stimulation of the mitogen-activated protein kinase pathway antagonizes TRAIL-induced apoptosis downstream of BID cleavage in human breast cancer MCF-7 cells. Oncogene 2002;21:4323–27.
42. Wolter KG, Hsu Y-T, Smith CL, Nechushtan A, Xi X-G, Youle RJ. Movement of Bax from the cytosol to mitochondria during apoptosis. J Cell Biol 1997;139:1281–92.
43. Kim JH, Ajaz M, Lokshin A, Lee YJ. Role of antitpoptotic proteins in Tumor Necrosis Factor-related Apoptosis-inducing Ligand and Cis-platin-augmented apoptosis. Clin Cancer Res 2003;9:3134–41.
44. Nam SY, Jung G-A, Hur G-C, Chung H-Y, Kim WH, Seol D-W, Lee BL. Upregulation of FLIPs by Akt, a possible inhibition mechanism of TRAIL-induced apoptosis in human gastric cancers. Cancer Sci 2003;94:1066–73.
45. Fulda S, Meyer E, Debatin K-M. Inhibition of TRAIL-induced apoptosis by Bcl-2 overexpression. Oncogene 2002;21:2283–94.
46. Franco AV, Zhang XD, Berkel EV, Sanders JE, Zhang XY, Thomas WD, Nguyen T, Hersey P. The role of NF-κB in TNF-related apoptosis-inducing ligand (TRAIL)-induced apoptosis of melanoma cells. J Immunol 2001;166:5337–45.

Laboratory Investigation

Oncology

Oncology 2006;70:25–33
DOI: 10.1159/000091183

Received: March 29, 2005
Accepted after revision: October 1, 2005
Published online: January 27, 2006

A New Specific Gene Expression in Squamous Cell Carcinoma of the Esophagus Detected Using Representational Difference Analysis and cDNA Microarray

Takatsugu Kan[a, b] Seiji Yamasaki[a] Kan Kondo[a] Naoki Teratani[a]
Atsushi Kawabe[a] Junichi Kaganoi[a] Stephen J. Meltzer[b]
Masayuki Imamura[a] Yutaka Shimada[a]

[a]Department of Surgery and Surgical Basic Science, Graduate School of Medicine, Kyoto University, Sakyo-ku, Kyoto, Japan; [b]Department of Medicine, Division of Gastroenterology, University of Maryland, School of Medicine and Greenebaum Cancer Center and Baltimore VA Hospital, Baltimore, Md., USA

Key Words
Representational difference analysis of cDNA · Esophageal squamous cell carcinoma · Human esophageal epithelial cell · LAGE-1 · HDAC inhibitor

Abstract
Objectives: To detect new specific gene expressions in squamous cell carcinoma of the esophagus. ***Methods:*** Representational difference analysis of cDNA (cDNA RDA) was applied to a human esophageal cancer cell line (KYSE170) and a human esophageal epithelial cell line (HEEC-1). ***Results:*** LAGE-1 was expressed specifically in KYSE170, but not in HEEC-1. It is also expressed in 27% of esophageal cancer cell lines (3/11) and 33% of esophageal cancer tissues (10/30), but not in other HEECs, normal esophageal epithelium, or other normal tissues except testis, ovary and kidney. The expression of LAGE-1 is strongly correlated with that of MAGE-A1 ($p = 0.013$, Fisher's exact probability test). Fibronectin, cytokeratin 6B, cytokeratin 19, cyclin D2 and Ten-m2 were detected as candidates for downregulated genes. Reduced expression profiles of them were also identified using cDNA microarrays. The expression of LAGE-1 was induced by 5′-aza-2′-deoxycytidine (5Aza-dC) and trichostatin A (TSA) in esophageal cancer cell lines, which did not express LAGE-1. In HEECs, 5Aza-dC induced LAGE-1 expression, but TSA did not. ***Conclusions:*** LAGE-1 expression was detected in esophageal cancer by cDNA RDA. LAGE-1 might have the potential to be a target antigen for anti-tumoral immunotherapy in esophageal cancers because of its tumor-specific expression similar to that of MAGE-A1.

Introduction

Esophageal cancer is known to have one of the worst prognoses among all cancers. For improving the poor prognosis of esophageal cancer, elucidation of the mechanism of tumor progression and applications of tumor-specific treatment strategies are needed. We employed representational difference analysis of cDNA (cDNA RDA [1]) to identify overexpressed or repressed esophageal cancer-specific genes. This approach has been used

KARGER
Fax +41 61 306 12 34
E-Mail karger@karger.ch
www.karger.com

0030–2414/06/0701–0025$23.50/0

Accessible online at:
www.karger.com/ocl

Yutaka Shimada, MD, PhD, FACS
Department of Surgery and Surgical Basic Science, Graduate School of Medicine
Kyoto University, Kawaracho 54 Shogoin Sakyo-ku, Kyoto 606-8507 (Japan)
Tel. +81 75 751 3626/3227, Fax +81 75 751 3626/4390
E-Mail shimada@kuhp.kyoto-u.ac.jp

to identify a number of new tumor-specific genes such as the MAGE [2], SAGE [3], BAGE [4], GAGE [5] and LAGE families [6], and CT10 [7]. These genes appear to be potential sources of antigens for cancer immunotherapy because they are expressed specifically in tumors of various histological types.

Recently, we established a protocol for culturing normal human esophageal epithelial cell lines (HEECs), and with those cell lines, we carried out gene expression profiling in human esophageal cancers using cDNA microarrays [8].

In the present study, we investigated the differences in gene expression between esophageal cancers and normal esophageal material using cDNA RDA and cDNA microarrays, and identified a candidate gene for cancer immunotherapy. Control mechanisms of genes that are specifically upregulated or downregulated in esophageal cancers were also examined.

Materials and Methods

Cell Lines and Tissues

Human esophageal cancer cell lines KYSE30, 150, 170, 410, 520, 590, 890, 960, 1190 and 2400, derived from squamous cell carcinoma [9], were grown in HAM/RPMI supplemented with 2% fetal calf serum, penicillin, and gentamicin. Other esophageal cancer cell lines, OE-33, KYAE and SKGT-4, derived from esophageal adenocarcinoma, were grown under the same conditions except in the case of OE-33, which was supplemented with 5% fetal calf serum. SUm/c that had been derived from squamous cell carcinoma of the esophagus floating in the thoracic duct was grown in culture medium with 5% fetal calf serum. HEEC-1, 2, 3 and 4, derived from the normal esophageal epithelium, were grown in Keratinocyte SFM (Invitrogen Corp., Carlsbad, Calif., USA)-containing supplements. The KYSE series, KYAE and HEECs were established in our laboratory, OE-33 was obtained from the European Collection of Cell Cultures (ECACC), and SKGT-4 and SUm/c were kindly donated by Dr. N. Altorki (Cornell University) and Dr. H. Watanabe (Tokyo, Japan), respectively. Specimens of normal and tumor tissues were obtained from our department under informed consent for all patients.

Preparation of cDNA

KYSE170 was derived from an esophageal cancer patient who had been alive for 12 years after surgery. Total RNA was extracted by the modified acid guanidinium thiocyanate-phenol-chloroform (AGPC) method from KYSE170 and from HEEC-1. Poly(A)+ RNA was purified using an Oligotex dT-30 super [poly(A) purification kit; Takara Bio Inc., Japan], according to the manufacturer's instructions. First-strand cDNA was synthesized by reverse transcription from 2 μg of each poly (A) + RNA sample (First strand cDNA Synthesis kit; Amersham Pharmacia Biotech, Bucks., UK). For double-stranded cDNA synthesis, 20 μl (total volume) of the first strand cDNA solution was mixed with 15 μl of 10× second strand buffer, 3 μl of dNTPs (10 m*M* each), 106 μl of H_2O, 1 μl of *E. coli* ligase (Invitrogen), 4 μl of *E. coli* DNA polymerase I (Invitrogen), and 1 μl of RNase H (Invitrogen), incubated at 16°C for 2 h, and then supplemented with 2 μl of T4 DNA polymerase (Invitrogen) and incubated at 16°C for another 2 h. Synthesized cDNA was phenol-extracted, ethanol-precipitated and resuspended in 20 μl of TE.

Protocol of cDNA RDA

The protocol for RDA as described by Hubank and Schatz [1] was used with some modifications. Two micrograms of each cDNA were digested with *Dpn* II (New England Biolabs, Beverly, Mass., USA). Twelve microliters (~1.2 μg) of digested cDNAs were ligated to R-Bgl adapters and amplified by PCR to generate the KYSE170 and HEEC-1 representations. The R-Bgl adapters were removed with *Dpn* II digestion, and the products (driver amplicon) were purified using spin columns: MICROCON YM-100 (Millipore Corp., Mass., USA) to remove impurities such as residual adapters and dNTPs. For tester representations, 2 μg of each driver amplicon were ligated to the J-Bgl adapters. Sequences of oligonucleotides used in cDNA RDA were as described in Lisitsyn and Wigler [10].

Hybridization and Selective Amplification

All steps were performed as described in Hubank and Schatz [1] with the following modifications: the tester (200 ng) to driver (20 μg) ratio for the first hybridization was 1:100. The tester (50 ng) to driver (40 μg) ratio for the second and third rounds was kept at 1:800. Most of the purification steps for products were performed using Microcon YM-100 (Millipore). Mung bean nuclease digestion before the last PCR in each RDA round was omitted.

Subcloning and Sequencing of Different Products

Subcloning steps were performed according to published protocols [1]. Briefly, the difference products of the second and third rounds were digested with *Dpn* II and purified by electrophoresis using a gel purification kit (Invitrogen), cloned into the *Bam* HI site of pBluescript KS$^+$ II (STRATAGENE Cloning Systems, La Jolla, Calif., USA), and transformed into DH-5 alpha (Invitrogen). White colonies were picked up from solid LB medium containing penicillin and X-gal (blue-white selection). Inserted fragments were checked by PCR using T3 and T7 primers and sequenced using an ABI Prism 377 DNA Sequencer (Applied Biosystems, Calif., USA). Sequence homology searches were performed in the databases provided by the National Center for Biotechnology Information (Bethesda, Md., USA) using the BLAST program [11].

Reverse Transcription-Polymerase Chain Reaction

Difference products obtained respectively from KYSE170 and from HEEC-1 as the tester were investigated by reverse transcription-polymerase chain reaction (RT-PCR) in KYSE170 and HEEC-1, respectively. Their expression was also examined in other esophageal cancer cell lines, in 8 surgically resected esophageal cancers (squamous cell carcinoma), in normal esophageal epithelial tissues, and in various other cancer cell lines and normal tissues (human tumor MTC panel and human MTC panels I & II; BD Clontech, Palo Alto, Calif., USA). PCR protocols were as follows: 35 cycles of 30 s at 95°C, 30 s at each optimal annealing temperature, and 1 min at 72°C. GAPDH was used as a positive control, and RNA was used as a negative control for RT-PCR of all speci-

mens in this study. The primer sequences of oligonucleotides used in RT-PCR designed using OLIGO™ primer analysis software and the annealing temperatures were as follows:

ERT: 5'-AGAAGAGCTGGAAGTGAG-3', 5'-ACCAAGTGGAGAAGAACA-3', 49°C,

PTI-1: 5'-GCTAAAAAGTGCCCGGAT-3', 5'-ACATTCAGTGCTCTACCC-3', 49°C,

LAGE-1: 5'-CCAAACACAAGGTCTCAG-3', 5'-ACAATGAACTGGCCACTC-3', 55.5°C,

fibronectin: 5'-ACTGCCAACTCTTTTACT-3', 5'-CTATTTCCTCCTGTTTCT-3', 51.9°C,

laminin: 5'-CCAAGACCCAGATCAACA-3', 5'-GGGTATTGTAGC AGCCTG-3', 53.7°C,

keratin 6B: 5'-CCTGAGAGCCTTGTATGA-3', 5'-AATCTCCTGCTTGGTGTT-3', 54°C,

keratin 19: 5'-GGCCTACCTGAAGAAGAA-3', 5'-ATTCTGCCGCTCACTATC-3', 56°C,

cyclin D2: 5'-GTGGTGCTGGGGAAGTTG-3', 5'-TCTGTAGGGGTGCTGGCT-3', 57°C,

Ten-m2: 5'-TGGGTG TGAATGTGTCTT-3', 5'-GAAGAAGGTGGACAGAGG-3', 53.2°C,

MAGE-A1, 5'-GCTGGAACCCTCACTGGGTTGCC-3', 5'-CGGCCGAAGGAAGGAACCTGACCCAG-3', 72°C,

GAPDH: 5'-TGGTATCGTGGAAGGACTCATGAC-3', 5'-ATGCCAGTGAGCTTCCCGTTCAGC-3', 50°C.

cDNA Microarray Analysis

Fourteen esophageal cancer cell lines (10 KYSE series, SUm/c, SKGT-4, OE-33, and KYAE) and 8 surgically resected esophageal cancer tissue samples (squamous cell carcinoma) were used for cDNA microarray analysis. The reference probes used for cancer cell lines and cancer tissues were HEECs and pooled normal esophageal epithelial tissues which had been obtained from the same surgical specimens. Details of the procedure were as previously described [8]. Briefly, 1 μg of mRNA was extracted from each sample. Cy3-dUTP and Cy5-dUTP were used for fluorescent labeling, and each sample of labeled first-strand cDNA was mixed and hybridized with Human Cancer Chip Version 2.0 (Takara Bio Inc.). Fluorescent images were examined using an Array Scanner 428 (Affymetrix, Inc., Santa Clara, Calif., USA), and the signal intensities calculated using ImaGene 3.0 (BioDiscovery Inc., Marina Del Rey, Calif., USA). For data analysis, we used publicly available clustering analysis software 'Cluster' and visualization software 'Tree View' [11].

Treatment with 5'-Aza-2'-Deoxycytidine and Trichostatin A

Four esophageal cancer cell lines (KYSE150, KYSE520, KYSE960 and SKGT-4) and 4 HEECs (HEEC-1–4) were grown in medium with various and continuous concentrations (0, 0.75, 2, 5 or 10 μ*M*) of 5'-aza-2'-deoxycytidine (5Aza-dC, Sigma Mo., St. Louis, Mo., USA) and with 100 μg/l, 500 μg/l, or 1 mg/l of tricostatin A (TSA, Sigma). Each medium had been replaced every day by fresh medium with the same concentration of 5Aza-dC and TSA until total RNA was isolated at various time points (1, 2 days, or 5 days). The expression levels of LAGE-1 were then investigated by RT-PCR as described above.

Results

Genes Overexpressed in an Esophageal Cancer Cell Line and a Human Esophageal Epithelial Cell Line

For detecting tumor-specific genes, an esophageal cancer cell line (KYSE170) was used as the source of tester cDNA against driver cDNA from a human esophageal epithelial cell line (HEEC-1). For detecting the downregulated genes in cancer cells, HEEC-1 was processed as the source of tester cDNA against driver cDNA from KYSE170. Tester and driver cDNAs were digested with a restriction enzyme (*Dpn* II), ligated to a pair of adapters, and then subjected to PCR amplification. The amplified tester was hybridized to a large excess of driver. The hybridization product was amplified by PCR using the tester-specific adapters as primers. Under these conditions, only tester-tester homoduplexes, corresponding to KYSE170- or HEEC-1-specific sequences, were amplified exponentially. This first difference product was submitted to two additional rounds of subtraction, digestion, and amplification that produced the second and third difference products. We examined the quality of difference products from each round of cDNA RDA by agarose gel electrophoresis. As shown in figure 1a, a stepwise reduction of complexity was seen in the three successive difference products and clear bands with little background were visible with ethidium bromide staining in the third difference product. Cloning of the second and the third difference products produced inserts whose sizes ranged from 120 to 300 bp, and sequence analysis of the genes revealed that there were 9 different genes. For tumor-specific genes, three difference products were obtained from KYSE170 (K-H-DP1~DP3); they were identified as LAGE-1, ERT (*Homo sapiens* Ets-related transcription factor), and PTI-1 (*Homo sapiens* prostate carcinoma tumor-inducing gene 1). For downregulated genes, six difference products were detected from HEEC-1 (H-K-DP1~DP6). They were identified as fibronectin, laminin, cytokeratin 19, cytokeratin 6B, cyclin D2, and ten-m2 (odd Oz/ten-m homolog 2) (table 1).

Expression of Esophageal Cancer-Specific Genes by RT-PCR

The patterns of expression of ERT, PTI-1, and LAGE-1 were checked because these genes were considered to be potential candidate genes that might be tumor-specific. All of these genes were expressed in KYSE170 but not in HEEC-1, which suggested that RDA in the current study worked properly. However, the ERT and PTI-1 genes were expressed in many esophageal cancer

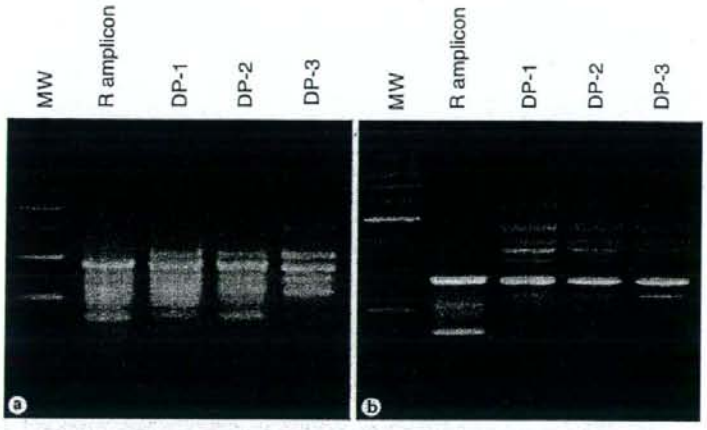

Fig. 1. Electrophoresis in 2% agarose gels with ethidium bromide staining of the final products from each round of cDNA RDA procedures. Molecular weight (MW), representative amplicon (R amplicon), difference product-1 (DP-1), DP-2 and DP-3 are shown from the left. Each band observed represents difference products. **a** KYSE170 vs. HEEC-1. KYSE170 was tester and HEEC-1 was driver. **b** HEEC-1 vs. KYSE170. HEEC-1 was tester and KYSE170 was driver.

Table 1. Three K-H-DPs and six H-K-DPs are shown

	Gene name	Length	Homology	Accession No.
K-H-DPs				
K-H-DP-1	LAGE-1	209 bp	100%	AJ223040
K-H-DP-2	ERT	189 bp	100%	AF017307
K-H-DP-3	PTI-1	301 bp	98%	L41498
H-K-DPs				
H-K-DP-1	fibronectin	181 bp	100%	X02761
H-K-DP-2	laminin	218 bp	99%	Z15008
H-K-DP-3	cytokeratin 19	278 bp	100%	Y00503
H-K-DP-4	cytokeratin 6B	262 bp	97%	BI335818
H-K-DP-5	cyclin D2	183 bp	99%	M90813
H-K-DP-6	odd Oz/ten-m homolog 2	153 bp	100%	NM_011856

All fragments turned out to have almost complete homology with known genes. Accession numbers represent genes in the GenBank database.

cell lines, all esophageal cancer tissues, and normal epithelial tissues of the esophagus (table 2). Both genes were also expressed in other normal tissues at a high rate (data not shown), which suggested that they were ubiquitously expressed. In contrast, LAGE-1 was expressed in 3/11 (27%) of esophageal cancer cell lines and 3/7 (43%) of esophageal cancer tissues, but was not expressed in normal epithelial tissues of the esophagus (table 2).

Expression of Genes Specifically Downregulated in Esophageal Cancer by RT-PCR

Nine genes identified from HEEC-1 when it was used as tester were examined as candidate genes representing the loss of normal genes in esophageal cancers. Fibronectin, laminin, cytokeratin 6B, and cytokeratin 19 were barely detected in KYSE170, but were distinctly detected in HEEC-1. In contrast, cyclin D2 and ten-m2 were detected in HEEC-1 but not in KYSE170. In additional examinations, laminin, cytokeratin 6B, and cytokeratin 19 were detected in most esophageal cancer cell lines and tissues, but cyclin D2 and ten-m2 were not detected in many esophageal cancer cell lines by RT-PCR (table 2).

cDNA Microarray Analysis

For comparison with the results from cDNA RDA, cDNA microarray analysis was performed. The DNA chips used in our microarray analysis did not have all genes that had been identified by cDNA RDA; neverthe-

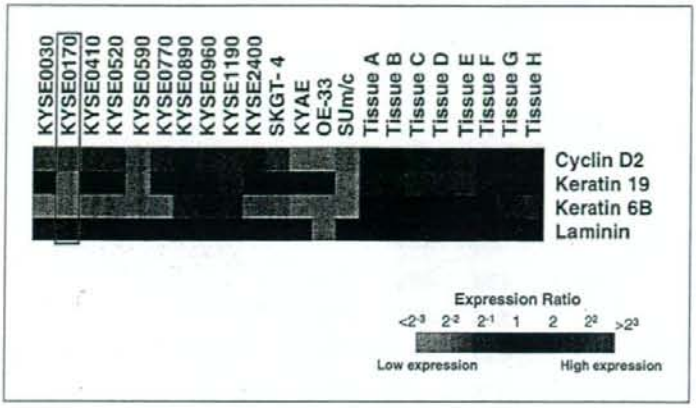

Fig. 2. cDNA microarray analysis for various esophageal cancer cell lines (squamous cell carcinomas; KYSE series and SUm/c, adenocarcinomas; SKGT-4, KYAE and OE-33) and esophageal cancer tissues (tissue A–H). The KYSE series includes KYSE 170, which was used as a driver in the current cDNA RDA (box).

Table 2. RT-PCR for various cell lines and tissue specimens

	KYSE170	HEEC-1	KYSE30	KYSE150	KYSE520	KYSE590	KYSE960	KYSE1190	SUm/c	SKGT-4	OE-33	KYAE	Tissue 1	Tissue 2	Tissue 3	Tissue 4	Tissue 5	Tissue 6	Tissue 7	*NT
LAGE-1	+	-	+	-	-	-	-	-	+	-	-	-	-	+	-	+	-	-	+	-
ERT	+	-	+	+	-	+	+	+	-	+	+	+	+	+	+	+	+	+	+	+
PTI-1	+	-	+	+	+	+	+	+	-	+	+	+	+	+	+	+	+	+	+	+
Fibronectin	+	+	+	+	+	+	-	+	+	+	+	-	+	+	+	+	+	+	+	+
Laminin	+	+	+	+	+	+	+	+	+	+	+	+	+	+	+	+	+	+	+	+
Cytokeratin 19	+	+	+	-	+	-	+	-	-	+	+	+	+	+	+	+	+	+	+	+
Cytokeratin 6B	+	+	+	+	+	+	+	+	+	+	-	+	+	+	+	+	+	+	+	+
Cyclin D2	-	+	-	+	-	-	-	-	+	-	-	-	+	+	+	+	+	+	-	+
ten-m2	-	+	-	-	-	-	+	+	-	-	-	-	+	-	+	+	+	+	+	+
GAPDH																				

All specimens were esophageal cancers except HEEC-1 and NT. * NT = Pooled sample of 10 normal tissues of esophagus. Tissue samples (tissue 1–7) were not identical to those in figure 2 (tissue A–H).

less, keratin 6B, keratin 19, laminin, and cyclin D2 were included. The expression of each of these genes obtained from cDNA microarrays was downregulated strongly in KYSE170 used as a driver (red box in fig. 2). These 4 genes were also found to be downregulated in most other esophageal cancer cell lines and esophageal cancer tissues (fig. 2).

Correlation between LAGE-1 and MAGE-A1

MAGE-A1 is known as one of the cancer/testis antigens and it has been reported that its expression was highly correlated with LAGE-1 [6]. For investigation of the correlation between these genes, the expression of LAGE-1 and MAGE-A1 in various specimens was examined by RT-PCR (table 3). The primers of MAGE-A1

Table 3. Comparison of LAGE-1 and MAGE-A1 by RT-PCR in various cancerous and normal specimens

Normal tissues	LAGE-1	MAGE-A1	GAPDH
Ovary	+	-	
Testis	+	+	
Kidney	+	-	
Small intestine	-	-	
Heart	-	-	
Prostate	-	-	
Brain	-	-	
Thymus	-	-	
Placenta	-	-	
Lung	-	-	
Liver	-	-	
Colon	-	-	
Muscle	-	-	
Pancreas	-	-	
Spleen	-	-	
Leukocyte	-	-	

Tumor samples (cancer cell lines)	LAGE-1	MAGE-A1	GAPDH
Prostatic adenocarcinoma	+	+	
Breast carcinoma	+	+	
Colon adenocarcinoma 1	-	+	
Colon adenocarcinoma 2	+	-	
Ovarian carcinoma	+	-	
Pancreatic adenocarcinoma	-	+	
Lung carcinoma (LX-1)	-	-	
Lung carcinoma (GI-117)	-	-	

Esophageal cancers	(positive/total)	
Esophageal cancer cell lines	3/11	6/11

Esophageal cancer tissues

LAGE-1	MAGE-A1	
	positive	negative
Positive	8	2
Negative	6	14

p = 0.013 (Fisher's exact probability test)

LAGE-1 was expressed in the kidney, ovary, and testis. MAGE-A1 was expressed in the testis. LAGE-1 and MAGE-A1 were also expressed in other cancer cell lines. Expression of LAGE-1 and MAGE-A1 was highly correlated in esophageal cancer cell lines and tissues.

used were the same as described in Hubank and Schatz [1]. LAGE-1 was not expressed in normal tissues except for testis, ovary, and kidney, and MAGE-A1 was expressed only in testis. LAGE-1 was expressed in 28% (3/11) of esophageal cancer cell lines and in 33% (10/30) of esophageal cancer tissues, while MAGE-A1 was expressed in 55% (6/11) and 47% (14/30), respectively. Moreover, the expression of LAGE-1 was strongly correlated with that of MAGE-A1 (p = 0.013, Fisher's exact probability test). The rate of expression of LAGE-1 among specimens in which MAGE-A1 was positive was 10/13 (77%).

Expression of LAGE-1 in Response to Treatment with 5Aza-dC or TSA

The expression of LAGE-1 induced by various continuous concentrations of 5Aza-dC and TSA for various incubation times is shown in table 4 A, B. 5Aza-dC was used at concentrations of 0.75, 2, 5 and 10 μM for treatment times of either 2 days or 5 days. For all HEECs, LAGE-1 expression was not induced after 2 days at any concentration of 5Aza-dC tested, but it was induced after 5 days of 5Aza-dC treatment at every concentration tested. In all esophageal cancer cell lines, LAGE-1 was also induced under certain conditions (table 4A). TSA was examined at continuous concentrations of 100, 500 and

Table 4. Induction of LAGE-1 expression by 5Aza-dC or TSA

A Expression by 5-Aza-dC

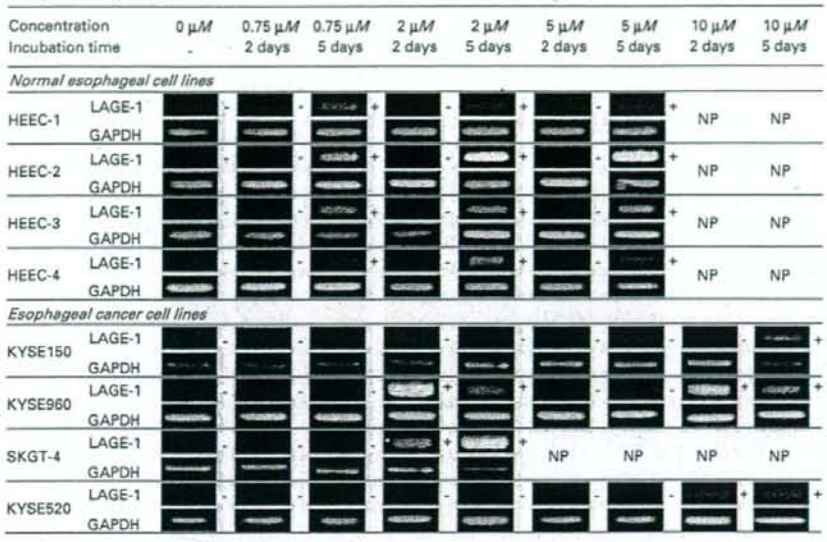

B Expression by TSA

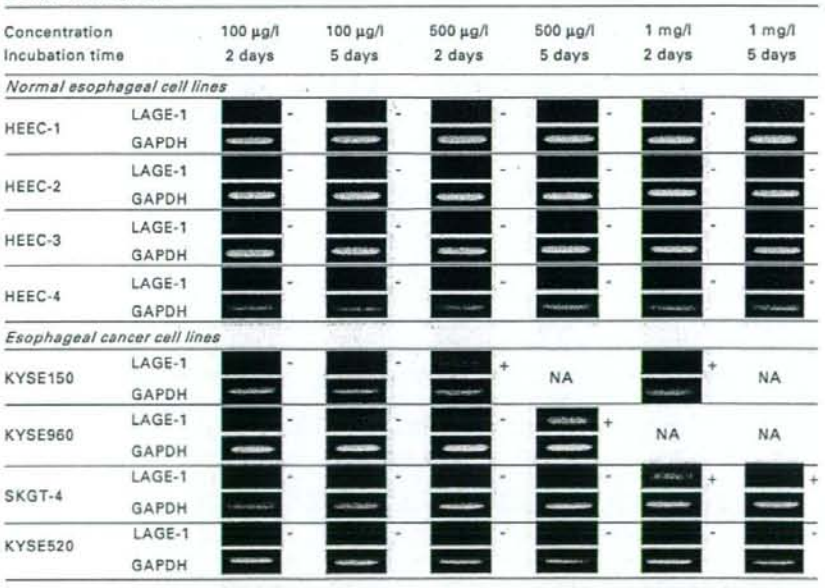

5Aza-dC induced LAGE-1 in all esophageal cancer and normal cell lines. TSA induced LAGE-1 in KYSE150, KYSE960 and SKGT4, but not in KYSE520 or any HEECs. NP = Not performed; NA = not available.

1 μg/l for treatment times of 1, 2 or 5 days. TSA induced LAGE-1 expression in KYSE150, KYSE960 and SKGT4, but not in any of the HEECs (table 4B). KYSE150 and KYSE960 were so sensitive for TSA that RNA could not be obtained in some experiments (shown as NA in table 4B).

Discussion

The original RDA method established by Lisityn et al. [10] is a high through-put method that can detect genomic amplification or deletion between two genomes by subtractive PCR. Hubank and Schatz [1] applied this genomic RDA protocol to cDNA, employed four-cutter restriction enzyme *Dpn* II, which increased the number of restriction sites, and consequently succeeded in obtaining more genetic information. We have modified this cDNA RDA protocol as described in Materials and Methods. (A) We omitted mung bean nuclease, because our results were not affected by whether mung bean nuclease was used or not (data not shown). (B) The tester-to driver ratio was fixed at 1:800 in the second and third steps. (C) spin column was used in all purification steps of PCR products for removal of residual adapters or dNTPs.

Using our cDNA RDA protocol, we detected the expression of several specific genes (LAGE-1, ERT, PTI-1, cyclin D2 and ten-m2) from esophageal squamous cell carcinomas and normal esophageal epithelial cell lines. Furthermore, using cDNA microarray analysis, we confirmed that the same expression patterns for fibronectin, keratin 6B, keratin 19, laminin, and cyclin D2 genes were obtained between cancer and the normal epithelium from esophageal cell lines or esophageal tissues. This strong correlation between the results from cDNA RDA and cDNA microarray analyses implies that cDNA RDA is still a simple and useful tool either for detecting new specific genes or for selecting genes that should be spotted in original microarrays because there are still a number of unknown genes that are merely predicted or sequenced although the human genome project is nearly finished.

Among the genes thus detected, ERT has been suggested to be a transcriptional factor involved in the transcriptional regulation of the transforming growth factor-β (TGF-β) type II receptor (RII) gene. PTI-1 is a genetic element expressed in specific human carcinomas and implicated in mutagenic changes in elongation factor 1α (EF-1 α) as a potential contributor to the carcinogenic process. These genes have been reported to encode transcription factors, suggesting that alteration of transcriptional control may directly contribute to cancer development and evolution [13–15]. Our data imply that these transcriptional factors were also upregulated in squamous cell carcinoma of the esophagus, suggesting that similar mechanisms of cancer development would probably apply to the esophagus.

Ten-m2, also called Odz, is a novel gene involved in directing segmentation in *Drosophila melanogaster* [16, 17]. This gene encodes a protein involved in signal transduction on the cell surface, rather than in transcription, and its function is related to cellular adhesion, involving interactions with NCAM, laminin, proteo-glycans, and integrins. The loss of ten-m2 in squamous cell carcinoma of the esophagus suggests its moderate adhesive potential and might increase the tendency toward distant metastasis. Hence, our data from cDNA microarray analysis were compatible with these characteristics of esophageal cancer.

LAGE-1 is 3,245 bp long in genomic DNA and encodes three exons [6]. LAGE-1a, 1b, 1L, and 1S are collectively known as LAGE-1 family genes. The fragment we identified had 100% homology to LAGE-1b and LAGE-1L [18]. Although NY-ESO-1 [19] is a member of the LAGE family, it belongs to LAGE-2, which is quite distinct from the LAGE-1 family of genes. In the present study, NY-ESO-1 was not detected in cell lines or tumor samples of the esophagus by RT-PCR, despite our usage of published primers and protocols (data not shown). Gene LAGE-1 has been mapped to Xq28 and is located close to the MAGE-A1 gene of the MAGE family. In this study, coincidental expression of LAGE-1 and MAGE-A1 was shown. The functions of these genes are still unknown, but some reports have suggested that they might regulate the expression of other genes [18]. It has been reported that epigenetic changes are related to the regulatory mechanisms of many genes, including MAGE-A1 and LAGE-1 [6]. There is no direct evidence in the articles reported that LAGE-1 is methylated. When we refer to the public database 'UCSC genome browser (http://genome.ucsc.edu/cgi-bin/hgGateway)' provided by the University of California, Santa Cruz, Calif., there are no reported CpG islands upstream of LAGE-1. LAGE expression was induced by 5-Aza-dC and TSA, suggesting that demethylation and histone acetylation may play important roles in the activation of this gene in tumors. The expression of LAGE-1 was more dependent on the duration of the incubation than the concentration of 5-Aza-dC in HEECs. In esophageal cancer cell lines, induction of the LAGE-1 gene by demethylation needed higher concentrations and longer durations. The involvement of his-

tone acetylation in the expression of LAGE-1 was also suggested to be quite different between HEECs and esophageal cancer cell lines. LAGE-1 was more inducible by TSA in some esophageal cancers than in HEECs. In each cell line, there may be variability in the ability of the components involved in acetylating mechanisms. Because of its tumor-specific expression similar to that of MAGE-A1, LAGE-1 has the potential to be a target antigen for anti-tumoral immunotherapy in esophageal cancers. In the near future, we should be able to improve the poor prognosis of esophageal cancer by vaccination utilizing such identified genes as antigens.

Acknowledgment

This research was partly supported by a grant from the Ministry of Education, Culture, Sports, Science and Technology (No. 13470234).

References

▶1 Hubank M, Schatz DG: Identifying differences in mRNA expression by representational difference analysis of cDNA. Nucleic Acids Res 1994;22:5640–5648.

▶2 De Plaen E, Arden K, Traversari C, Gaforio JJ, Szikora JP, De Smet C, Brasseur F, van der Bruggen P, Lethe B, Lurquin C, et al: Structure, chromosomal localization, and expression of 12 genes of the MAGE family. Immunogenetics 1994;40:360–369.

▶3 Martelange V, De Smet C, De Plaen E, Lurquin C, Boon T: Identification on a human sarcoma of two new genes with tumor-specific expression. Cancer Res 2000;60:3848–3855.

▶4 Boel P, Wildmann C, Sensi ML, Brasseur R, Renauld JC, Coulie P, Boon T, van der Bruggen P: BAGE: a new gene encoding an antigen recognized on human melanomas by cytolytic T lymphocytes. Immunity 1995;2:167–175.

▶5 Van den Eynde B, Peeters O, De Backer O, Gaugler B, Lucas S, Boon TA: new family of genes coding for an antigen recognized by autologous cytolytic T lymphocytes on a human melanoma. J Exp Med 1995;182:689–698.

▶6 Lethe B, Lucas S, Michaux L, De Smet C, Godelaine D, Serrano A, De Plaen E, Boon T: LAGE-1, a new gene with tumor specificity. Int J Cancer 1998;76:903–908.

▶7 Gure AO, Sockert E, Arden KC, Boyer AD, Viars CS, Scanlan MJ, Old LJ, Chen Y: T. CT10: a new cancer-testis (CT) antigen homologous to CT7 and the MAGE family, identified by representational-difference analysis. Int J Cancer 2000;85:726–732.

▶8 Kan T, Shimada Y, Sato F, Maeda M, Kawabe A, Kaganoi J, Itami A, Yamasaki S, Imamura M: Gene expression profiling in human esophageal cancers using cDNA microarray. Biochem Biophys Res Commun 2001;286:792–801.

▶9 Shimada Y, Imamura M, Wagata T, Yamaguchi N, Tobe T: Characterization of 21 newly established esophageal cancer cell lines. Cancer 1992;69:277–284.

▶10 Lisitsyn N, Wigler M: Cloning the differences between two complex genomes. Science 1993; 259:946–951.

▶11 Altschul SF, Madden TL, Schaffer AA, Zhang J, Zhang Z, Miller W, Lipman DJ: Gapped BLAST and PSI-BLAST: a new generation of protein database search programs. Nucleic Acids Res 1997;25:3389–3402.

▶12 Eisen MB, Spellman PT, Brown PO, Botstein D: Cluster analysis and display of genome-wide expression patterns. Proc Natl Acad Sci USA 1998;95:14863–14868.

▶13 Saeki H, Kuwano H, Kawaguchi H, Ohno S, Sugimachi K: Expression of ets-1 transcription factor is correlated with penetrating tumor progression in patients with squamous cell carcinoma of the esophagus. Cancer 2000;89:1670–1676.

▶14 Shen R, Su ZZ, Olsson CA, Fisher PB: Identification of the human prostatic carcinoma oncogene PTI-1 by rapid expression cloning and differential RNA display. Proc Natl Acad Sci USA 1995;92:6778–6782.

▶15 Choi SG, Yi Y, Kim YS, Kato M, Chang J, Chung HW, Hahm KB, Yang HK, Rhee HH, Bang YJ, Kim SJ: A novel ets-related transcription factor, ERT/ESX/ESE-1, regulates expression of the transforming growth factor-beta type II receptor. J Biol Chem 1998;273:110–117.

▶16 Oohashi T, Zhou XH, Feng K, Richter B, Morgelin M, Perez MT, Su WD, Chiquet-Ehrismann R, Rauch U, Fassler R: Mouse ten-m/Odz is a new family of dimeric type II transmembrane proteins expressed in many tissues. J Cell Biol 1999;145:563–577.

▶17 Ben-Zur T, Feige E, Motro B, Wides R: The mammalian Odz gene family: homologs of a Drosophila pair-rule gene with expression implying distinct yet overlapping developmental roles. Dev Biol 2000;217:107–120.

▶18 Aarnoudse CA, van den Doel PB, Heemskerk B, Schrier PI: Interleukin-2-induced, melanoma-specific T cells recognize CAMEL, an unexpected translation product of LAGE-1. Int J Cancer 1999;82:442–448.

▶19 Chen YT, Scanlan MJ, Sahin U, Tureci O, Gure AO, Tsang S, Williamson B, Stockert E, Pfreundschuh M, Old LJ: A testicular antigen aberrantly expressed in human cancers detected by autologous antibody screening. Proc Natl Acad Sci USA 1997;94:1914–1918.

J. Biochem. **139**, 697–703 (2006)
doi:10.1093/jb/mvj086

Ultrasensitive DNA Chip: Gene Expression Profile Analysis without RNA Amplification

Kunihisa Nagino*,†, Osamu Nomura†, Yuki Takii†, Akira Myomoto†, Makiko Ichikawa†, Fumio Nakamura†, Masashi Higasa†, Hideo Akiyama†, Hitoshi Nobumasa†, Satoshi Shiojima‡ and Gozoh Tsujimoto‡

New Frontiers Research Laboratories, Toray Industries, Inc., Kanagawa 248-8555; and Department of Genomic Drug Discovery Science, Graduate School of Pharmaceutical Sciences, Kyoto University, Kyoto 606-8501

Received October 30, 2005; accepted February 8, 2006

We have developed a new DNA chip whose substrate has a unique minute columnar array structure made of plastic. The DNA chip exhibits ultrahigh sensitivity, up to 100-fold higher than that of reference DNA chips, which makes it possible to monitor gene expression profiles even with very small amounts of RNA (0.1–0.01 μg of total RNA) without amplification. Differential expression ratios obtained with the new DNA chip were validated against those obtained with quantitative real-time PCR assays. This novel microarray technology would be a powerful tool for monitoring gene expression profiles, especially for clinical diagnosis.

Key words: agitation, columnar array structure, DNA chip, microarray, sensitivity.

The Completion of the Human Genome project has significantly accelerated functional genomic studies. Nowadays, DNA microarrays, such as a DNA chip, are being used for high-throughput analysis. Microarray technology has recently been shown to be the most useful among many functional genomic approaches (*1–5*). Moreover, the DNA chip is promising to be a powerful tool not only for genetic diagnosis (*6–10*) but also for personalized therapy (*3*).

Generally speaking, there are two dominant methods for immobilizing oligonucleotides on a substrate for DNA chips; one is the direct synthesis of nucleic acids step by step on the solid substrate, and the other is the immobilization of synthesized oligonucleotides on the solid substrate using a high speed robot. The advantage of the photolithography method is the mass production of high-density DNA chips on which high-density oligonucleotides are immobilized. On the other hand, it requires special facilities and many photomasks to prepare the DNA chips, resulting in high cost. Taking genetic diagnosis with DNA chips into account, made-to-order DNA chips containing selected DNA probes for individual patients will be required for personalized therapy. From the viewpoint of personalized therapy, the DNA chips prepared by the second method are preferable.

However, most current DNA chips are not applicable for clinical use because of their low sensitivity. Assersohn *et al.* (*11*) reported that the mean recovery of breast fine needle aspirate was 202,500 cells, which corresponds to approximately 0.1 μg of total RNA. In general, a large amount of total RNA (1–100 μg) is required for a DNA chip (*12*). For example, the Affymetrix GeneChip prepared by the photolithography method operates with 1–15 μg of total RNA with a single round cDNA synthesis. Analysis of the gene expression profile in a small amount of sample using current DNA chip technology requires RNA amplification (*15–17*), which may lead to biased results (*18, 19*). If only a small amount of sample, such as a biopsy one, is available for the assay, gene expression analysis of the sample is difficult using the existing DNA chips.

Here, we succeeded in highly sensitive detection of hybridization signals using our newly developed DNA chip having a unique structure made of plastic. The level of nonspecific adsorption of target DNA was reduced and the signal intensity of hybridization was increased on the DNA chip, hence the signal/noise (S/N) ratio was remarkably improved. Moreover, our DNA chip makes it possible to perform gene expression profiling with 0.1 μg of total RNA without any amplification. This performance strongly suggested that our new DNA chip would be useful for genetic diagnosis.

MATERIALS AND METHODS

Oligonucleotides—In most experiments, 64 different 70 bases oligonucleotides selected from a commercially available oligonucleotide set (QIAGEN, Human sample set, ver. 3.0) were used as DNA probes. In some experiments (Table 1 and Fig. 8), a 60 bases oligonucleotide (sequence, 5′-ACATTTTGAGGCATTTCAGTCAGTTGCTCAATGTACCTATAACCAGATCGTTCATCTGGA) complementary to plasmid pkF3 (Takara Bio) was used. A 20 bases oligonucleotide (sequence, 5′-TGGAGAACTTGATCGACAAG) was also used (Fig. 7). All oligonucleotides were chemically modified with an amino group at the 5′-terminal.

New DNA Chip—Substrate: A poly (methyl methacrylate) (PMMA) substrate, 76 × 26 × 1 mm, was used as the substrate for our newly developed DNA chip. This substrate has a unique structure, as shown in Fig. 1. A depressed structure with 256 arrayed pillars is located at the center of the substrate. The diameter of the top of the pillars is 0.15 mm, and their height is 0.2 mm. The DNA

*To whom correspondence should be addressed. E-mail: Kunihisa_nagino@nts.toray.co.jp
†Present address: Toray Industries, Inc.
‡Present address: Kyoto University.

Table 1. **Effect of bead agitation on hybridization signal intensities with the new DNA chip.** The target DNA originated from the pKF3 plasmid.

Concentration of DNA (ng/μl)	0.15	0.3	0.75
With agitation	2,020	2,470	4,510
Without agitation	660	770	1,400
Ratio of (with agitation)/ (without agitation)	3.1	3.2	3.2

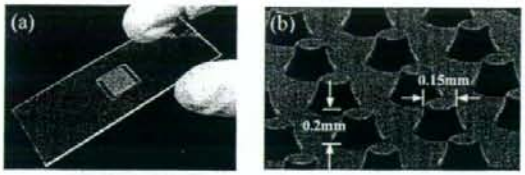

Fig. 1. **(a) Photograph of the new DNA chip and (b) magnified SEM image of pillars at the center of the substrate.**

chip substrate is manufactured by injection molding. Figure 1 (a and b) shows a photograph and a SEM image of this chip substrate, respectively. The oligonucleotides were covalently immobilized on the upper surface of the pillars according to the following procedure.

Surface treatment and oligonucleotide immobilization: The side chain of PMMA was hydrolyzed in an aqueous 1 N sodium hydroxide solution to produce carboxyl groups on the surface. 5′-Amino–modified oligonucleotides, dissolved in an aqueous solution at 30 μM, were spotted onto the upper surface of the pillars robotically using Gene STAMP II (Nippon Laser & Electronics Lab.). The solution ("spotting solution") comprised 100 mM 2-morpholinoethanesulfonic acid, pH 7.0 (MES, Sigma), 500 mM NaCl, 50 mg/ml 1-ethyl-3-(3-dimethylaminopropyl) carbodiimide (EDC, Dojindo), and 0.005% (w/v) sodium dodecylsulfate (SDS, Sigma). After spotting, the substrate was incubated for 16 h in a 100% humidity chamber at 37°C and then washed with Milli-Q water. The oligonucleotides were immobilized the entire tops of the pillars through amide bonds. Figure 7b shows the reaction scheme.

Reference DNA Chip—Reference DNA chips were fabricated using commercially available glass slides (SDA0011; Matsunami Glass Industries, Ltd.). The 5′-amino–modified oligonucleotides described above were dissolved in Solution-I (Takara-Bio) at 30 μM and then spotted robotically. After spotting, the glass slides were incubated for 16 h in a humid chamber and then immersed for 20 min in a blocking solution (DBL0500; Matsunami Glass Industries, Ltd.). The glass slides were washed twice with Milli-Q water and once with ethanol, and then dried.

Target DNAs—In most experiments, target DNAs were prepared as described below: Total RNAs extracted from human brain and liver were purchased from BD Biosciences Clontech. Cy3 (Brain)- and Cy5 (liver)-labeled cDNAs were synthesized by reverse transcription from total RNAs using a CyScribe First-Strand cDNA Labeling Kit (RPN6200; Amersham Biosciences), according to the manufacturer's instructions.

In some experiments (Fig. 7), a chemically synthesized 20-mer oligonucleotide (sequence, 5′-CTTGTCGATCAAGTTCTCCA; Cy3-labeled at 5′-terminal) was used. A labeled DNA originating from pKF3 was also used in place of the target DNA (Table 1 and Fig. 8). The latter was prepared as follows: A pKF3 template was amplified by PCR (primer sequences: 5′-GGGCGAAGAAGTTGTCCATA-3′ and 5′-GCAGAGCGAGGTATGTAGGC-3′). The PCR conditions were as follows: initial 94°C for 4 min, and them 94°C for 40 s, 59°C for 1 min, 72°C for 1 min; 35 cycles. All PCR experiments were conducted with PCT-200 (MJ Research). The PCR products were purified by ethanol precipitation, dissolved in 40 μl of water and then heat-denatured. Next, 2 μl of a random 9 bases primer (6 mg/ml), 5 μl of 10× Klenow buffer, 2.5 μl of a dNTP mixture (2.5 mM each dATP, dTTP and dGTP, and 400 μM dCTP), 2 μl of Cy3-dCTP (Amersham Bioscience), and 10 U of Klenow fragment (2140A; Takara Bio) were added to the DNA solution. The mixture was incubated for 4 h at 37°C and the labeled product was purified by ethanol precipitation.

Hybridization—For the new DNA chip, we devised a special hybridization method to enhance the hybridization fluorescence signal. Briefly, a 20 × 20 mm transparent plastic cover with two through-holes, 0.8 mm in diameter and at opposite corners, was bonded to the center portion of the substrate with double-coated adhesive tape (No. 532; Nitto Denko Co., Ltd.). Figure 2 shows illustrations of the new DNA chip. The target DNA was dissolved in 40 μl of hybridization solution; this solution was applied to the center of the new DNA chip through the holes using a micropipette. About 0.5 mg of micro-glass beads, 125 μm in diameter, suspended in the hybridization solution, was also applied to the center of the new DNA chip in the same way. The hybridization solution comprised 5× SSC (saline-sodium-citrate; Sigma), 0.1% (w/v) SDS, 1% (w/v) BSA (bovine serum albumin; Sigma), and 0.01% (w/v) salmon sperm DNA (Sigma). The holes were sealed with adhesive tape. Beads added to the hybridization solution were driven between the convex-concave structures of the new DNA chip, which agitated the hybridization solution. The beads moved in the concave portion of the new DNA chip without scratching the upper surface of the pillars whereon the oligonucleotides were immobilized.

For reference DNA chips, the target DNA was dissolved in 30 μl of hybridization solution. A 50 × 20 mm cover glass (CG00014; Matsunami Glass Industries, Ltd.) was placed on the spotted area of the slide glass, and then the target DNA solution was applied.

Both the new and reference DNA chips were incubated for 16 h at 42°C. For the new DNA chip, the hybridization solution was agitated by movement of the beads during the hybridization. After the hybridization, the covers were removed, and the chips were washed with 3× SSC containing 0.1% SDS, 1× SSC and 0.1× SSC sequentially at room temperature, and then dried with a spin drier. Hybridization signals were scanned using a DNA chip scanner (GenePix 4000B; Axon Instruments).

Quantitative Real-Time PCR Analysis—Real-time RT-PCR (TaqMan) analysis was carried out using an ABI Prism 7000 Sequence Detector System (Applied Biosystems), according to the manufacturer's instruction. TaqMan probes (Assay-on-Demand) were purchased from Applied Biosystems.

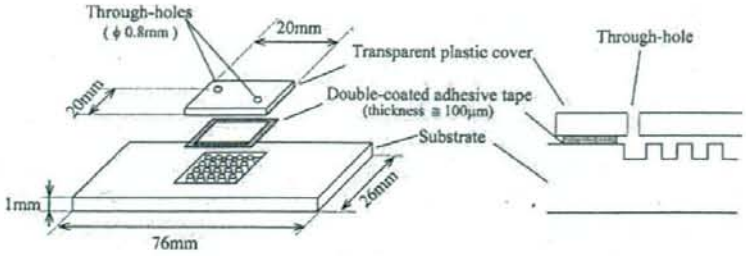

Fig. 2. **Schematic illustrations of the new DNA chip; the right one shows a side view of the chip.**

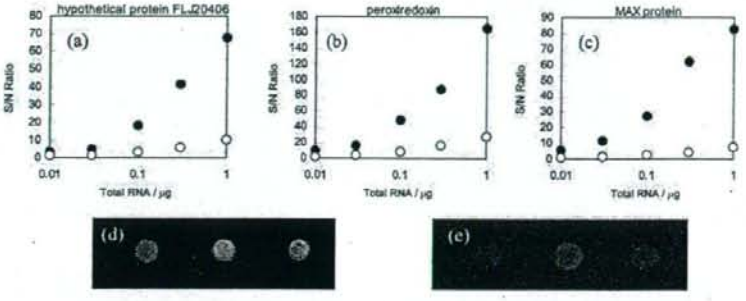

Fig. 3. **S/N ratios and fluorescence images of the new and reference DNA chips after hybridization.** The S/N ratios for the new (solid circles) and reference (open circles) DNA chips for three selected genes are shown in (a), (b) and (c). Fluorescence images of the new (d) and reference (e) DNA chips (amount of total RNA, 0.1 μg) are also shown. In each image, the spots represent hypothetical protein FLJ20406, peroxiredoxin and MAX protein from the left.

Table 2. **Signal intensities obtained with the new and reference DNA chips (amount of total RNA, 0.1 μg).**

Gene name	Serine/ threonine kinase 24	Peroxiredoxin	MAX protein
Signal intensity of new DNA chip	1,070	4,010	2,220
Signal intensity of reference DNA chip	510	1,500	520
Ratio of (new DNA chip)/ (reference DNA chip)	2.1	2.7	4.3

RESULTS AND DISCUSSION

We first examined the agitation effect on the hybridization efficiency using the new chip. Table 1 shows the concentration dependence of the hybridization efficiency with and without agitation of the solution by beads.

The hybridization signals in both cases decreased with decreasing concentration of the target DNA. This result indicates that the agitation with the beads increased the hybridization signals to more than three times compared with no agitation. In the case of no agitation, the low signal intensity was due to the low diffusion constant (D) of the target DNA in the solution. The diffusion constant of 25 bases oligonucleotides is reported to be 8×10^{-8} cm^2/s (*20*). Therefore, the mean square distance of the target DNA in 16 h is calculated to be 0.0092 cm^2, and the average migration distance is 0.096 cm. This average migration distance indicates that only a 1.5% of the target DNA in the hybridization solution is accessible to the probe DNAs on the pillars without agitation under our conditions, assuming the area of hybridization assay is 4 cm^2.

In the next step, the signal intensities obtained with the new DNA chip were compared with those obtained with the reference DNA chip. Three oligonucleotides were selected from the commercially available oligonucleotide set (hypothetical protein FLJ20406, peroxiredoxin and MAX protein). After synthesizing a Cy3-labeled cDNA from 5 μg of total RNA, 0.1 μg of cDNA was applied to the new DNA chip as well as to the reference DNA chip. As shown in Table 2, the new DNA chip showed a markedly higher signal intensity sensitivity, approximately 2–4 times fold higher, than the reference DNA chip.

Next, we examined the signal-to-noise (S/N) ratio of the new DNA chip compared with that of the reference DNA chip because not only enhancement of the signal but also control of the background noise is important for the development of new DNA chip. In most cases, the noise mainly comes from nonspecific adsorption of target DNA onto the substrate. Figure 3 (a, b and c) shows the S/N values obtained with three kinds of target DNA. The results indicate that the new DNA chip showed a markedly higher S/N ratio, approximately 20–100 fold higher, than the reference DNA chip. That is to say, the new DNA chip required small amounts of target DNA (1/20–1/100) to show an equivalent S/N ratio to in the case of the reference DNA chip.

Figure 3 (d and e) shows fluorescence images of the new and reference DNA chips after hybridization. These images clearly indicate the new DNA chip gives higher signals and lower noise compared to the reference chip. In the case of Fig. 3 (d and e), the S/N ratio for the new DNA chip was approximately 5–10 fold higher than that for the reference DNA chip. The high S/N ratios of the new DNA chip were obtained by enhancing the signal level as well as by reducing the noise level. In the case of the new DNA chip, the

noise level was 60–70% lower than that for the reference DNA chip (data not shown). The enhanced signal level was predominantly due to the bead agitation. The markedly reduced noise was due to three reasons. The first reason is the new chip's unique structure. Table 3 shows the relationship between defocus and noise intensity on untreated substrates. As we expected, the noise decreases in the background area when the focal point is adjusted to the top of the pillar. Practically, the noise decreased to 60% when the defocus distance was 200 μm. The second reason is that PMMA exhibits low autofluorescence. Table 3 shows the comparison of the noise of due to PMMA and the slide glass used for the DNA chips. The noise mainly comes from the autofluorescence of the substrates. The noise of PMMA is less than that of the glass substrate. The last reason is surface charges on the substrate. Unreacted carboxyl groups might remain on the surface after the reaction, as shown Fig. 7. Because the carboxyl group shows negative charge at neutral conditions, repulsive forces might exist between the negatively charged target DNA and the surface, resulting in less nonspecific adsorption of the target DNA during the hybridization assay.

Table 3. **Relationship between defocus and the noise level on untreated substrates.**

Defocus (μm)	0	50	100	200
PMMA substrate	330	250	190	180
Glass slide (SDA0011)	460	–	–	–

Next, we investigated whether our DNA chip is applicable to gene expression analysis with a small amount of target DNA. Cy3- and Cy5-labeled cDNAs synthesized from the total RNA (1 to 0.01 μg) from human brain and liver, respectively, were used as target cDNAs. Fluorescence images of the new and reference DNA chips after hybridization are shown in Fig. 4. As shown in Fig. 4, all the hybridization signals obtained using the new DNA chip were markedly higher and had lower noise compared to with the reference DNA chip. In particular, when the amount of total RNA was 0.1 or 0.01 μg, most signals were difficult to detect for the reference DNA chip, while signals on most spots were clearly observed with the new DNA chip. Figure 5 shows scatter plots of the new and reference DNA chips with different amounts of total RNA. The new DNA chip showed a wide dynamic range even when the amount of total RNA was 0.1 or 0.01 μg.

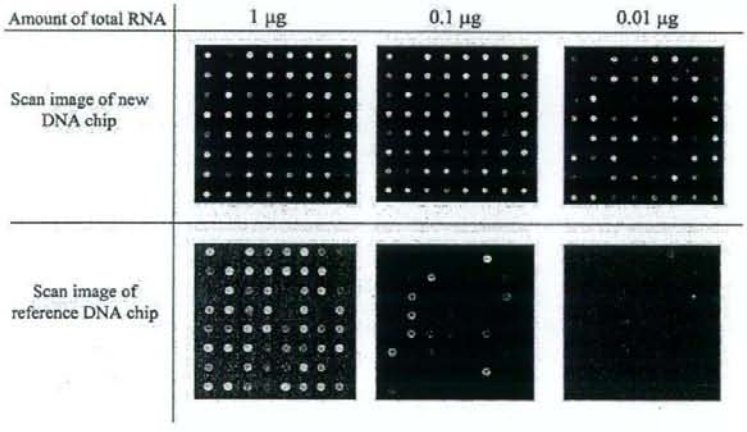

Fig. 4. **Scan images of the new and reference DNA chips.**

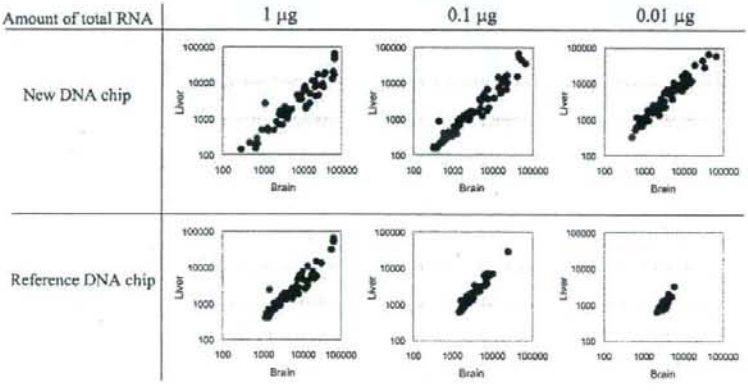

Fig. 5. **Scatter plots of the new and reference DNA chips with different amounts of total RNA.**

On the other hand, the dynamic range of the reference DNA chip became narrower as the amount of total RNA decreased. In the next step, we examined the Cy3/Cy5 ratio to confirm the reliability of the new DNA chip. The analysis was performed with different amounts of total RNA (1 and 0.1 μg, 1 and 0.01 μg). The correlation coefficients obtained with using the new and reference chips are summarized in Table 4. The values for the new chip are obviously superior to those for the reference chip. In particular, the correlation coefficient for the new chip was 0.80 even when 0.01 μg of total RNA was used, while it was 0.10 with the reference chip. Additionally, the correlation coefficient between the new and reference DNA chips was 0.88 in the case of 1 μg of total RNA.

These results shows that our DNA chip makes it possible to perform gene expression profiling with only 0.1 μg of total RNA without any amplification. Moreover, it is strongly suggested that our DNA chip has the ability to monitor gene expression profiles even with an amount of total RNA as low as 0.01 μg.

Table 4. **Correlation coefficients of Cy3/Cy5 ratios with different amounts of total RNA.**

Amounts of total RNA (μg)	1 and 0.1	1 and 0.01
New DNA chip	0.87	0.8
Reference DNA chip	0.49	0.1

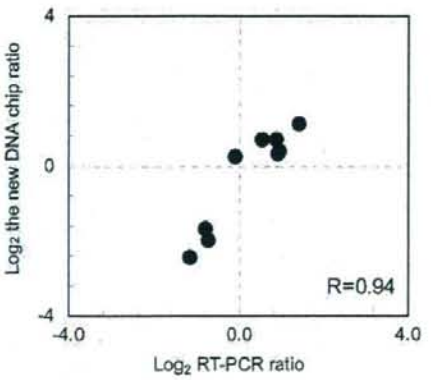

Fig. 6. **Correlation of differential expression ratios (stomach cancer/stomach) for the new DNA chip and RT-PCR (TaqMan).**

To determine the correlation between the signals and the amounts of expressed RNAs, the differential expression ratios obtained with the new DNA chip were compared with those obtained on quantitative real-time PCR analysis. For this analysis, we selected nine genes that are differentially expressed between two human RNA samples (stomach cancer and stomach; BD Bioscience Clontech): HLA-F, PARVB, NR2C1, MDH1, MTI1E, RPL23AP7, BRDT, CD84 and SERPINA1. 5′-Amino-modified 70 bases oligonucleotides originating from the nine genes were chemically synthesized and immobilized on the substrate as described above. The cDNAs hybridized to the new DNA chip were produced from 1 μg of total RNAs. As shown in Fig. 6, the correlation coefficient for both results was 0.94, which is higher than the reported values [0.79–0.92 (*21*)] obtained with a commercially available DNA chip. This result indicates that the new DNA chip can be accurately used to monitor the gene expression ratios in samples.

In this study, we used PMMA as the substrate. PMMA has following the advantages: Firstly, substrates with unique structures can be easily manufactured by means of injection molding. Secondly, it exhibits low autofluorescence. Thirdly, a simple surface modification is available, as shown in Fig. 7b. Although some PMMA surface modification methods have been reported (*22–25*), these methods have a disadvantage, *i.e.*, the PMMA surface tends to be adversely affected by organic solvents or reagents. Here, the question arose as to whether the PMMA substrate contributed to the ultrahigh sensitivity of the new DNA chip. To address this question, the following experiment on the material effect on the sensitivity was carried out. To introduce carboxyl groups onto a glass surface, aminosilane-coated slides (S8111; Matsunami Glass Industries, Ltd.) were immersed in 1-methyl-2-pyrrolidone containing 1.6% (w/v) succinic anhydride (Sigma) and 2.3% (v/v) borate buffer (100 mM, pH 8.0) for 20 min, rinsed with Milli-Q water and then dried (*26*). A 60-mer oligonucleotide composed of a sequence complementary to the target DNA, dissolved in the spotting solution at 30 μM, was spotted robotically and immobilized on glass and PMMA plates with amide binding. The procedures for the reactions are shown in Fig. 7. The target DNA was synthesized from the pKF3 template by the random priming method. The size of the target DNA was estimated to be 200–300 bases on electrophoretic analysis. The hybridization signals on glass and PMMA are shown in Fig. 8, which clearly indicates that the signal intensity on PMMA is superior to that on glass. Although it is not clear why the higher signal intensity was observed in the case of PMMA, we propose

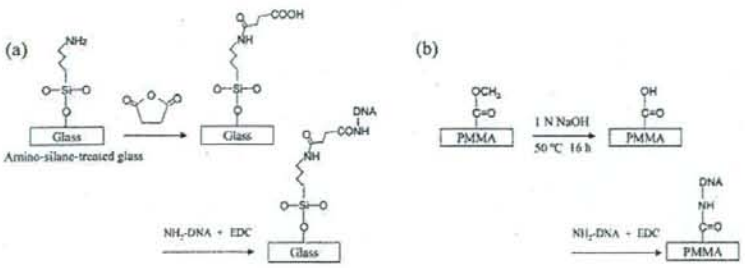

Fig. 7. **Schematic representation of the procedures for immobilization of oligonucleotide on glass (a) and PMMA (b).**